Eur. Phys. J. B **48**, 501–508 (2005)
DOI: 10.1140/epjb/e2006-00009-1

THE EUROPEAN PHYSICAL JOURNAL B

Formation dynamics of bipolaron in a metal/polymer/metal structure

Y.H. Yan[1], Z. An[1,2], C.Q. Wu[1,a], and K. Nasu[3]

[1] Department of Physics, Fudan University, Shanghai 200433, P.R. China
[2] College of Physics, Hebei Normal University, Shijiazhuang 050016, P.R. China
[3] Institute for Materials Structure Science, KEK, Tsukuba, Ibaraki 305-0801, Japan

Received 25 June 2005
Published online 19 January 2006 – © EDP Sciences, Società Italiana di Fisica, Springer-Verlag 2006

Abstract. Charge injection process from metal electrode to a nondegenerate polymer in a metal/ polymer/ metal structure has been investigated by using a nonadiabatic dynamic method. We demonstrate that the dynamical formation of a bipolaron sensitively depends on the strength of applied electric field, the work function of metal electrode, and the contact between the polymer and the electrode. For a given bias applied to one of the electrode (V_0) and coupling between the electrode and the polymer (t'), such as $V_0 = 0.79$ eV and $t' = 1$ eV, the charge injection process depending on the electric field can be divided into the following three cases: (1) in the absence of the electric field, only one electron tunnels into the polymer to form a polaron near the middle of the polymer chain; (2) at low electric fields, two electrons transfer into the polymer chain to form a bipolaron; (3) at higher electric fields, bipolaron can not be formed in the polymer chain, electrons are transferred from the left electrode to right electrode through the polymer one by one accompanying with small irregular lattice deformations.

PACS. 73.40.Ns Metal-nonmetal contacts – 71.38.Mx Bipolarons – 72.80.Le Polymers; organic compounds (including organic semiconductors)

1 Introduction

Conducting polymers have attracted much interest for its commercial applications, e.g., organic light emitting diodes, solar cells, etc. [1,2]. Understanding mechanisms of the electron injection from metal electrodes into organic material is of great importance for improving the performance of these organic-based devices. Due to the strong electron-lattice interactions, it is well known that additional electrons or holes in conducting polymers will induce self-localized excitations, such as solitons [3] (only in *trans*-polyacetylene), polarons and bipolarons [4]. As a result, it has been generally accepted that the charge carriers in conjugated polymers are these excitations including both charge and lattice distortion [5]. The formation and transport of such carriers are believed to be of fundamental importance.

Both polarons and bipolarons, which are composite particles with internal structure, can be formed in nondegenerate conjugated polymers, such as poly-(phenylenevinylene) and polythiophene. The bipolarons are spinless species with charge $\pm 2|e|$, in contrast to the spin-bearing polarons (spin 1/2, charge $\pm|e|$). Therefore, the properties of the transport and the recombination of bipolarons will be much different from that of polarons. The existence of bipolarons is likely to play an important role in understanding the operation of these optoelectronic devices based on conjugated polymers. There have been considerable amounts of research works devoted to the properties of bipolarons, for example, the formation and stability of bipolaron [6–9], the infrared-active vibrational modes (IRAV modes) around a bipolaron [10,11], and the bipolaron lattice at metal-polymer interface [12]. However, most of these works were focusing on the static properties of bipolarons. Apparently, the injection of charge from electrodes, the transport of charge carriers, and the recombination of oppositely charged polarons and/or bipolarons, are dynamical processes accompanying with both charge motion and lattice distortion driven by applied electric field. Therefore, a real-time dynamical model should be much appropriate for the simulations of these processes.

The lattice dynamics [13–23] has been widely used to simulate the formation of these nonlinear elementary excitations induced by photoexcitations or charge injections, and their motion driven by applied electric field, within the tight-binding Su-Schrieffer-Heeger(SSH) model [3] as well as its extended versions for nondegenerate polymers [4]. For example, it has been shown that the photocarriers (charged polarons) are generated directly by

[a] e-mail: cqw@fudan.edu.cn

photoexcitations with a quantum yield about 25% [13]. Importantly, the formation mechanism of charged polarons can only be understood within the dynamical scheme. In the presence of an external electric fields, solitons as well as polarons keep their shape while moving along a polymer chain. Solitons are shown to have a maximum velocity $2.7v_s$, where v_s is the sound velocity [14, 15]. The situation is different for polarons, which has been shown to be not created in electric fields over 6×10^4 V/cm due to the charge moving faster and not allowing the distortion to occur [16]. In a recent work by our group [17], the charge injection from metal electrode into a degenerate polymer chain has been investigated, where the highest occupied molecular orbit (HOMO) is arranged to be singly occupied for observing the formation of singly charged polaron. It has been found that the dynamical formation of a polaron sensitively depends on the strength of applied electric field. Additionally, there are other studies on the charge injection through metal/polymer interfaces, e.g., the resistance of organic molecular wires attached to metallic surface [24], Schottky energy barriers in metal/organic [25,26], tunnelling of charge carrier into polaron level in polymer [27], and the dynamics of charge transport in a short oligomer sandwiched between two metal contacts [28]. However, to our knowledge, the dynamical formation of a bipolaron remains to be investigated.

It is the aim of this study to describe the formation process of a bipolaron in a metal/polymer/metal structure. In this paper, we present our results from a nonadiabatic dynamical study of both lattice relaxation and charge motion induced by charge injection from metal electrode to polymer chain in the presence of an external electric field. The polymer chain considered here has a nondegenerate geometry, in which bipolarons can be created. The dynamics is treated within the mean-field approximation, where transitions between instantaneous eigenstates are allowed, in contrast to the adiabatic dynamics with fixed level occupation [23]. The paper is organized as follows. In the following section, we present a tight-binding one-dimensional model for the metal/polymer/metal structure and describe the nonadiabatic dynamical evolution method. The results will be discussed in Section 3. Finally, a summary is given in Section 4.

2 Model and method

We consider a one-dimensional metal/polymer/metal structure that contains a nondegenerate polymer chain as well as two metal electrodes attached to its two ends. The Hamiltonian consists of three parts,

$$H = H_e + H_{latt} + H_{ex}. \tag{1}$$

The electronic part is

$$H_e = -\sum_n t_n (c_{n+1}^\dagger c_n + \text{h.c.}), \tag{2}$$

t_n being the hopping integral between sites n and $n+1$, that is, $t_n = t_0$ in the two metal electrodes, $t_n = t_0 - \alpha(u_{n+1} - u_n) + (-1)^n t_e$, where u_n is the monomer displacement of site n, α describes the electron-lattice coupling between neighboring sites in the polymer chain, such as the SSH model, t_e is the Brazovskii-Kirova symmetry-breaking term for describing nondegenerate polymer [4], and $t_n = t'$ for the coupling between sites connecting the polymer chain and the electrodes. $c_n^\dagger$ (c_n) creates (annihilates) an electron at site n. The polymer lattice is described by

$$H_{latt} = \frac{K}{2}\sum_n (u_{n+1} - u_n)^2 + \frac{M}{2}\sum_n \dot{u}_n^2, \tag{3}$$

where K is the elastic constant and M the mass of a CH group. The contribution from the external field is

$$H_{ex} = \sum_n V_n(t)\left(c_n^\dagger c_n - 1\right), \tag{4}$$

$V_n(t)$ being site energy due to the applied voltage bias and electric field. At the left metal electrode a voltage bias is applied for the charge injection, $V_n(t) = V(t)$. At the polymer chain a uniform electric field $E(t)$ along the $-\hat{\mathbf{x}}$ is applied, $V_n(t) = -|e|E(t)[(n-n_0)a + u_n]$, where e being the electron charge, n_0 the first site of the polymer chain, and a is the lattice constant. At the right metal electrode, a field-free area, the site energies $V_n(t)$ are chosen as $V_{n_1}(t)$, n_1 is the last site of the polymer chain. The spin index in the electron operators is omitted since the electron interaction will not be considered here.

We consider a finite system containing a 200-monomer polymer chain and two 100-site metal electrode at the two ends. The model parameters are those generally chosen for polyacetylene [5]: $t_0 = 2.5$ eV, $\alpha = 4.1$ eV/Å, $K = 21$ eV/Å^2, $M = 1349.14$ eV fs^2/Å^2, $t_e = 0.05$ eV, and $a = 1.22$ Å. The coupling between the polymer and metal is set to be $t' = 0.4\ t_0$. Before we go further for the dynamical evolution, we determine the lattice configuration and the structure of the energy levels in the absence of external field [$V(t) = 0$ and $E(t) = 0$] in this section.

The total energy is obtained by the expectation value of the Hamiltonian (1) at the ground state $|g\rangle$,

$$E_{tot} = \langle g|H_e + H_{ex}|g\rangle + \frac{K}{2}\sum_n (u_{n+1} - u_n)^2. \tag{5}$$

The electronic states are determined by the electronic part of the Hamiltonian (1), and the lattice configuration of the polymer $\{u_n\}$ is determined by the minimization of the total energy in the above expression,

$$u_{n+1} - u_n = -\frac{\alpha}{K}(\rho_{n,n+1} + \rho_{n+1,n}) + \lambda, \tag{6}$$

where λ is the Lagrangian multiplier to guarantee the polymer chain length unchanged, i.e., $\sum_n (u_{n+1} - u_n) = 0$. $\rho_{m,n}$ is the element of the density matrix, which will be given below.

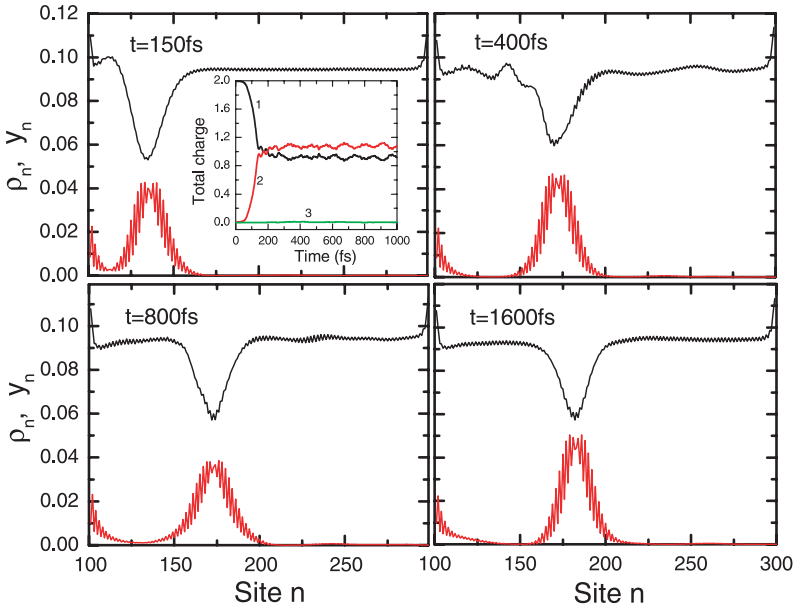

Fig. 1. Charge distribution ρ_n and the staggered lattice configuration y_n of the polymer chain at different times in the absence of electric field. $V_0 = 0.79$ eV. The inset shows the total charge evolution with 1, 2 and 3 denoting metal (L), polymer, and metal (R), respectively.

Now, we describe the nonadiabatic dynamic method that has been used for the dynamics of soliton and polaron in an electron-lattice interacting system. The evolution of the electron wave functions depends on the time-dependent Schrödinger equation

$$i\hbar\dot{\Psi}_k(n,t) = -t_n\Psi_k(n+1,t) - t_{n-1}\Psi_k(n-1,t) + V_n(t)\Psi_k(n,t), \quad (7)$$

where the site index n runs over the whole chain. The lattice displacements are determined by the following Newtonian equations of motion:

$$M\ddot{u}_n = -K(2u_n - u_{n+1} - u_{n-1}) + 2\alpha Re[\rho_{n,n+1} - \rho_{n-1,n}] + |e|E(t)[\rho_{n,n} - 1], \quad (8)$$

where n runs only in the polymer sites. $\rho_{m,n}$, the element of the density matrix, is defined as

$$\rho_{m,n}(t) = \sum_k \Psi_k(m,t) f_k \Psi_k^*(n,t), \quad (9)$$

where f_k is the time-independent distribution function determined by initial occupation (being 0,1 or 2). The coupled differential equation (7) and (8) can be solved numerically by the Runge-Kutta method. A small damping is also introduced to obtain a more realistic behavior of the system [22,29].

In the real calculation, we choose the external field to be turned on smoothly, viz., we let $V(t) = V_0 \exp[-(t - t_c)^2/t_w^2]$ for $0 < t < t_c$ and $V(t) = V_0$ for $t \geq t_c$, with t_c being a smooth turn-on period and t_w the width. As the voltage bias $V(t)$, the applied electric field $E(t)$ is also turned on smoothly, i.e., $E(t) = E_0 \exp[-(t - t_c)^2/t_w^2]$ for $0 < t < t_c$ and $E(t) = E_0$ for $t \geq t_c$, with the same t_c and t_w. In the simulation, we take $t_c = 75$ fs, $t_w = 25$ fs, and various values of voltage bias V_0 and electric field.

3 Results and discussions

First of all, we present our results on the charge injection in the absence of external fields by increasing the voltage bias, which can be considered as the metal work function [17]. Although the electronic states in the polymer and the metal electrodes are mixed, due to the coupling between the polymer and the metal electrodes, it can be clearly distinguished to be in the polymer or the metal electrodes, by calculating the wave-function possibilities $\eta_\mu^{(\kappa)} (\equiv \sum_{n\in\kappa} |\Psi_\mu(n)|^2)$ for each state μ, where $\Psi_\mu(n)$ is the wave function at site n and κ is a set of sites (the left metal electrode, the polymer chain, or the right metal electrode) [17]. At the initial state ($V_0 = 0$), the polymer chain is dimerized with an energy gap of about $E_g = 1.76$ eV, as same as that for an isolate polymer chain. The highest occupied molecular orbit (HOMO) of the metal electrodes lies naturally at the Fermi level at the middle of the gap. In this case, no charge can be injected into the polymer chain due to the larger energy barrier. Then, we increase the voltage bias V_0 applied at the left electrode step by step, which raise its energy levels by a value of about V_0 while the energy levels in the other parts are almost unchanged. It has been shown that the system will be unstable and charges start to be injected into the polymer through the metal/polymer interface when the highest occupied electronic state of the left metal electrode is close to the bottom of the conduction band due to the applied voltage bias ($V_0 \geq 0.78$ eV).

In Figure 1, we show the charge distribution $\rho_n [\equiv \rho_{n,n} - 1]$ and the lattice configuration y_n $[\equiv (-1)^n(u_{n+1} - u_n)]$ at a few typical times for the case that a voltage bias $V_0 = 0.79$ eV is applied, which is just above the minimal value ($V_{min} \approx 0.78$ eV) for the charge injection in the absence of the electric field. Different from our

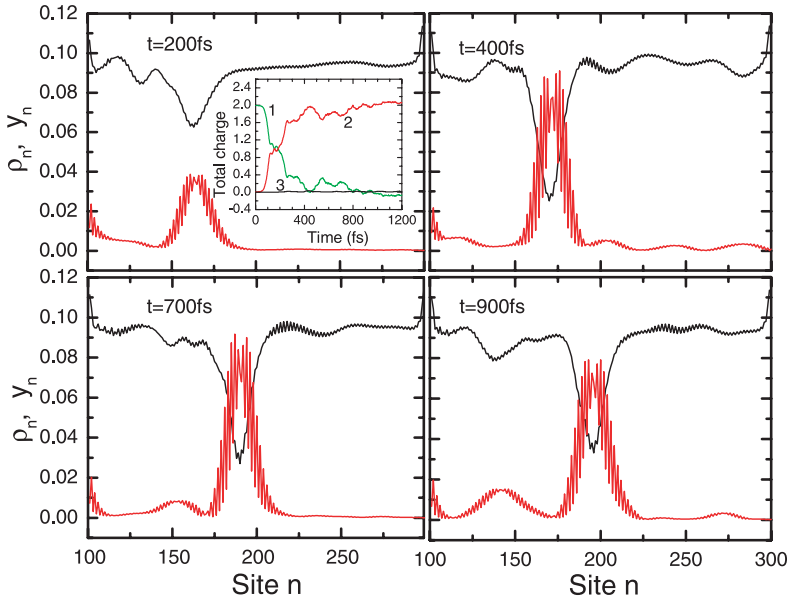

Fig. 2. Charge distribution ρ_n and the staggered lattice configuration y_n of the polymer chain at different times in the absence of electric field. $V_0 = 0.81$ eV. The inset shows the total charge evolution with 1, 2 and 3 denoting metal (L), polymer, and metal (R), respectively.

previous work where an extra electron is put on the lowest unoccupied state of the left metal electrode [17], here, we have arranged two extra electrons on the lowest unoccupied state of the left metal electrode for observing the formation of an bipolaron. As the bias is turned on smoothly, the energy of the HOMO at the left electrode, $E_{\rm HO}$ goes up towards the bottom of the conduction band. At 75 fs, $E_{\rm HO}$, reaches its maximum value, 0.87 eV, which is very close to the bottom of the conduction band, 0.88 eV. As a consequence, the coupling between electronic states of the left metal electrode and the polymer becomes strongest due to the less energy difference, the extra electrons initially on the left metal begin to move into the polymer gradually. From Figure 1, one can observe that the charge injection takes place within 150 fs which is much shorter than the time of polaron formation in the degenerate polymer chain [17]. Due to the interaction with the left interface, the charge will move very slowly towards the center of the polymer chain. Finally, around $t = 1600$ fs, a stable charged polaron state forms near the 180th site. From the inset, it can be found that about one electron charge is injected to polymer and a small amount of charge, about $0.12|e|$, is distributed on some sites near the left interface in the polymer chain. The charge distributed on the distortion lattice sites in the middle of the polymer chain is nearly one, which is just the charge of a perfect polaron. This implies that the charge is injected into the polymer one by one, not as expected that the total two extra charges will be injected at the same time. We also observe that the charge injection takes place within about 150 fs, then the total charge of the polymer chain oscillates around a balance value due to the bouncing out and back of the charge from the left interface.

However, when we increase further the voltage bias, it shows different charge injection from that for the above case. For example, Figure 2 shows the charge distribution ρ_n and the lattice configuration y_n at a few typical times for the case that a voltage bias $V_0 = 0.81$ eV is applied. It can be found that about one electron charge is injected into the polymer chain within 150 fs, and a charged polaron is generated near the 160-th site. Nevertheless, this only lasts a small period, about several tens of femtoseconds. Then, another electron is transferred from the left metal electrode into the polymer chain between 200 fs and 400 fs. A bipolaron, in which two electrons are trapped, is formed. As expected, it is implied that the larger voltage bias applied on the left metal, i.e., the work function of metal electrode, favors electron injection, and that a bipolaron can be created by two electrons injected into polymer. However, one can find, for another time, that the two charges are not transferred at the same time, but injected one by one.

Moreover, we have also investigated the charge injections at larger coupling constants between the electrode and the polymer chain (t'). The larger coupling constant represents that the contact between the electrode and the polymer is stronger. As a example, Figure 3 shows the charge distribution ρ_n and the staggered lattice configuration y_n of the polymer chain at various times in the absence of the electric field ($V_0 = 0.79$ eV) for $t' = 0.64\ t_0$. One can find that a bipolaron is formed directly, within a few hundreds of femtoseconds. From the inset, one can find that more than two electron charges, about $2.3|e|$, are injected into the polymer chain very fastly, within 100 fs. Two electrons are trapped in the bipolaron state, and a small amount of charges lies at the interface. Comparing with the weaker coupling case (Fig. 1), it is shown that the good contact can facilitate the charge injection, as expected.

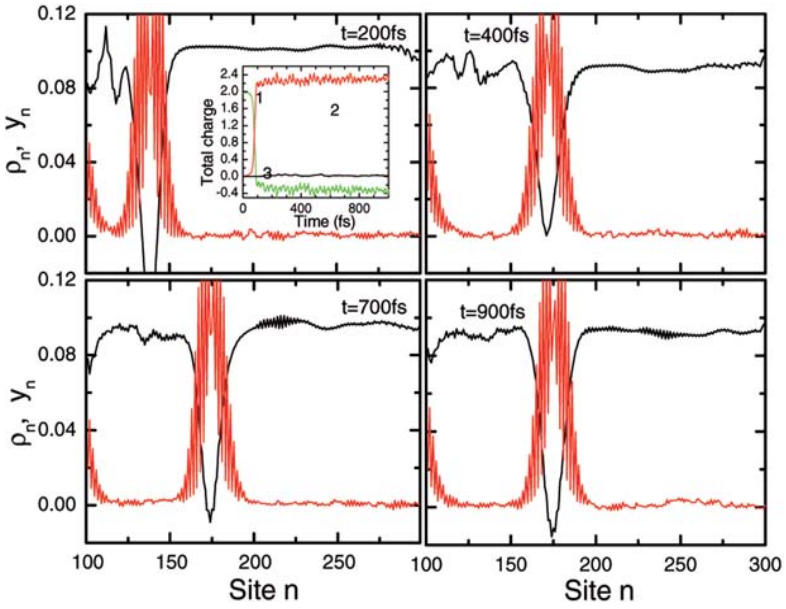

Fig. 3. Charge distribution ρ_n and the staggered lattice configuration y_n of the polymer chain at different times in the absence of the electric field with the coupling constant $t' = 0.64\ t_0$ and $V_0 = 0.79$ eV. The inset shows the total charge evolution with 1, 2 and 3 denoting metal (L), polymer, and metal (R), respectively.

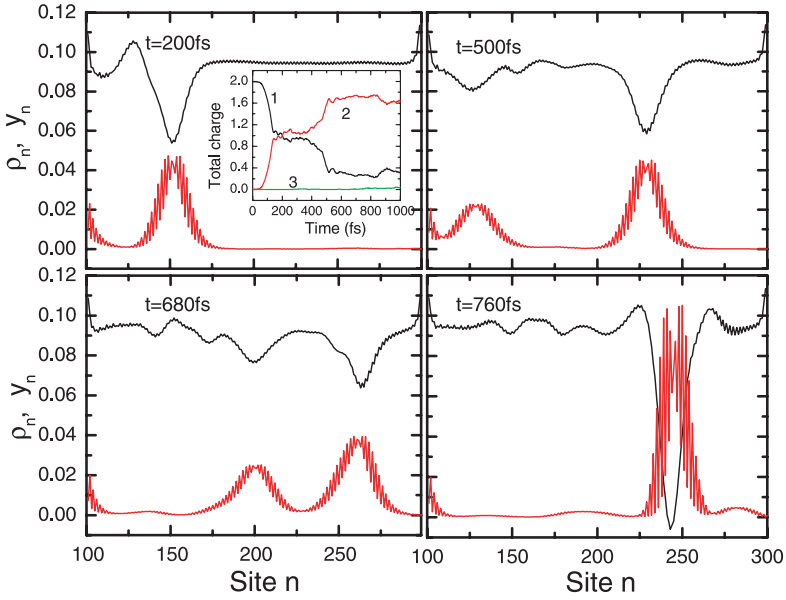

Fig. 4. Charge distribution ρ_n and the staggered lattice configuration y_n of the polymer chain at different times under the electric field $E_0 = 0.05$ mV/Å. $V_0 = 0.79$ eV. The inset shows the total charge evolution with 1, 2 and 3 denoting metal (L), polymer, and metal (R), respectively.

Now, we present the behavior of charge injection through the metal/polymer interface under an applied electric field, for a given bias applied to the left metal electrode (V_0) and coupling between the electrode and the polymer (t'), such as $V_0 = 0.79$ eV and $t' = 0.4\ t_0$. In the case of a weak electric field, for example, $E_0 = 0.05$ mV/Å, the evolution of both the charge distribution ρ_n and the lattice configuration y_n is shown in Figure 4. We observe that a polaron forms at about $t = 200$ fs, and then it moves towards the right interface under the electric field. At about $t = 500$ fs, while the formed polaron reaches at about 230-th site, another charge enters into the polymer chain through the left interface, and induces lattice distortion to form a small polaron. This newly formed polaron will chase the previously formed one. At $t = 680$ fs, around 220-th site, the two polarons meet and begin to combine. Finally, a bipolaron forms at about $t = 760$ fs as sketched by Figure 4. The time from the two polaron encountering to being combined completely is estimated to be 80 fs. Comparing with the results in the absence

of external field, it is indicated that the applied field reduces effectively the potential barrier and favors charge injection. The inset shows the total charge evolution in different segments. From the inset, one can find that after about one electron charge is injected, the polymer chain undergoes a relaxation process of about 210 fs (from 150 fs to 360 fs), then another electron is injected from 360 fs to 520 fs. After that, the total charge exhibits an oscillation behavior due to the charge scattering on the left interface. Furthermore, one can find that the charge does not enter the right metal electrode, which shows that the electric field is too weak to overcome the barrier at the right polymer/metal interface.

As a comparison, the formation process of a bipolaron from two negative charged polarons is depicted in Figure 5 The top three panels show the lattice configuration and the charge distribution of three typical times, and the lowest panel presents three energy eigenvalues evolution of conduction band bottom. Two initial negative charged polarons are separated by 60 sites, which corresponds to just several sites overlap of the wave functions of polarons. As time evolves, the two polarons get closer and closer. Around $t = 90$ fs, the two polarons combine completely to form a bipolaron. At the same time, the two polaron energy levels, initially very close, are bifurcated: one goes up to the conduction band, the other becomes deeper to form a bipolaron energy level. The time of the bipolaron formation, about 90 fs, is very close to that of the above case if we take into account the electric field effect in the latter one. When the initial two polarons are separated by an even larger distance, say, 80 sites, the wave functions of the two polarons overlap little, it takes much long time, about 280 fs for the two polarons to combine completely. Whereas the two polarons are 40 sites apart, it takes about 40 fs for the polarons to combine.

Charge injection process under a little higher electric field, $E_0 = 0.5$ mV/Å, is showed in Figure 6. Unlike the case of $E_0 = 0.05$ mV/Å, we do not observe the formation process of a bipolaron resulting from the combination of two polarons formed at different time. Instead, we find that the charge gradually accumulates to form a bipolaron at the right interface within 600 fs. From the inset, we observe that at 550 fs, the total charge in the polymer chain reaches its maximum value, less than two electron charges. The reason is that a small amount of charge, about $0.3|e|$, has been transferred into the right metal electrode through the right interface. From about 360 fs, the charge in the polymer chain begins to move into the right metal electrode. This can be understood that the electric field reduces the barrier of the charge jumping through the interface [17]. Therefore, the existence time of the bipolaron is very short as compared to the case of $E_0 = 0.05$ mV/Å. It is very interesting to note that an amount of charge held by the bipolaron is continually transferred into the right metal electrode, but about one electron is left in the polymer chain between 700 fs and 1100 fs, which indicates the bipolaron has changed to a polaron. This implies that charges are transferred from the polymer into the electrode one by one, similar as the

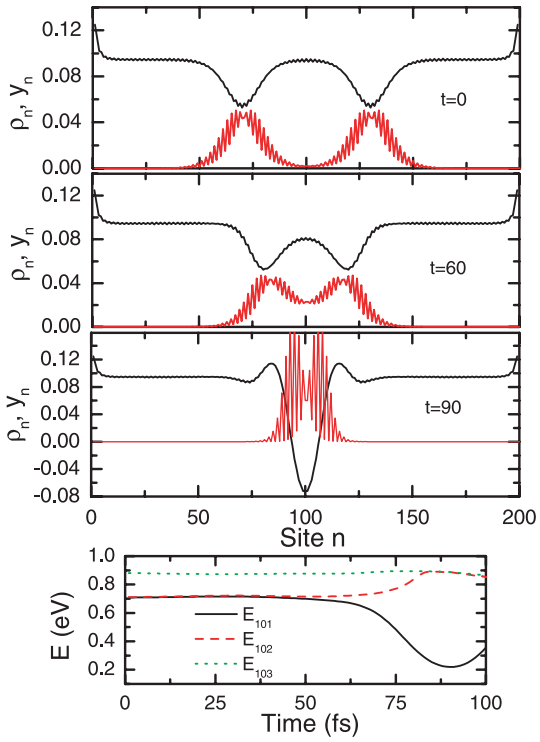

Fig. 5. Charge distribution ρ_n and the staggered lattice configuration y_n of the polymer chain at different times and the evolution of eigenenergy levels with time.

case that charges are injected to the polymer. Eventually, a small amount of charge kept in the polaron enters into the right metal electrode, and about $0.5|e|$ is left in the polymer chain to induce some irregular lattice oscillations.

Figure 7 depicts the charge injection process under a even higher electric field, $E_0 = 1$ mV/Å. In this case, we do not observe a bipolaron formation clearly, but some irregular lattice deformations. Accompanying with these irregular lattice deformations, two separated charge envelopes can be found between 300 fs and 700 fs (see the panel at $t = 400$ fs), but only one is left (see the panel at $t = 800$ fs). From the inset, it can be found that electrons are injected into the polymer chain continually, and the charge in the polymer chain reaches its maximum value, about $1.6|e|$, at $t = 430$ fs, then decreases accompanying with some oscillations. Meanwhile, we observe charge increase in the right electrode. The result indicates that the electric field applied at the polymer chain reduces effectively the potential barriers at the polymer/metal interfaces. The charge injected into the polymer chain from the left metal electrode is rapidly transferred to the right metal electrode, thus, the localized lattice deformation, such as polaron and bipolaron, can not be formed. Therefore, our results implies that the external electric field is disadvantageous for the formation of a bipolaron. At last, it should be stressed that the oscillation behavior should arise from the reflection of charge between the two metal electrodes.

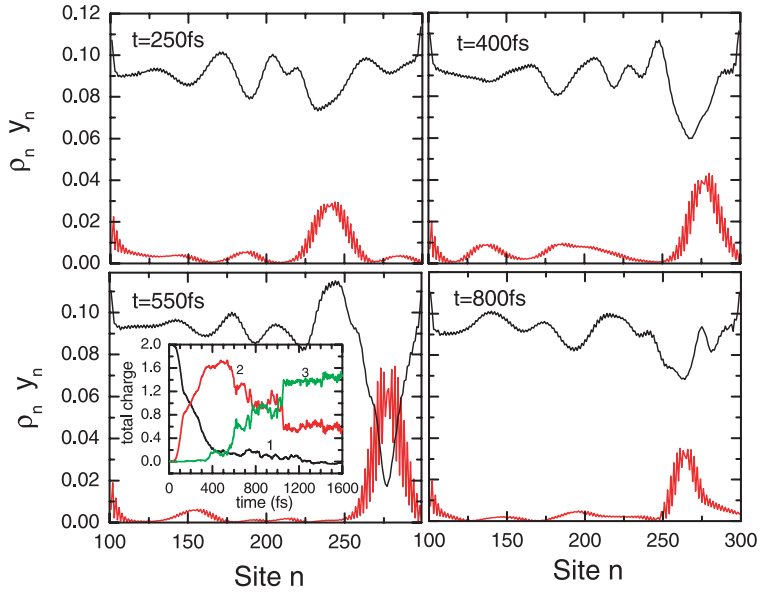

Fig. 6. Same as in Fig. 1 but with electric field $E_0 = 0.5$ mV/Å. The inset shows the total charge evolution with 1, 2 and 3 denoting metal (L), polymer, and metal (R), respectively.

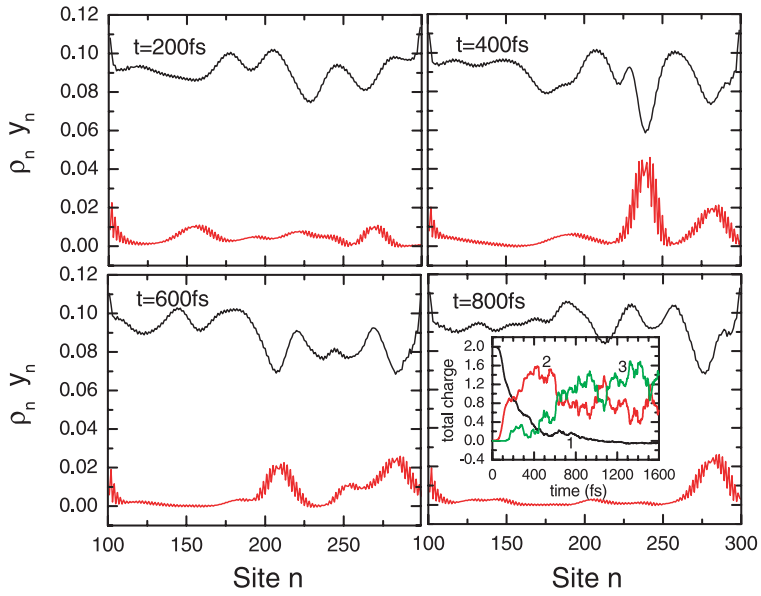

Fig. 7. Same as in Figure 1 but with electric field $E_0 = 1$ mV/Å and $V_0 = 0.79$ eV. The inset shows the total charge evolution with 1, 2 and 3 denoting metal (L), polymer, and metal (R), respectively.

4 Summary

In summary, we have investigated the bipolaron formation from point contact in a metal/polymer/metal structure by using a nonadiabatic dynamic method based on the time-dependent Schrödinger equation for the electronic wave function combining the Newtonian equation of the motion for the polymer monomer displacement. It has been shown that the dynamical formation of a bipolaron sensitively depends on the strength of applied electric field, the work function of metal electrode, and the contact between the polymer and the electrode. The larger voltage bias applied on the metal electrode, i.e., the work function of metal electrode, favors electron injection, and facilitates the formation of bipolaron. Similarly, the good contact can facilitate the charge injection and the formation of bipolaron. For a given bias applied to one of the electrode(V_0) and coupling between the electrode and the polymer (t'), such as $V_0 = 0.79$ eV and $t' = 1$ eV, the charge injection process depending on the electric field can be divided into the following three cases: (1) in the absence of the electric field, only one electron tunnels into the polymer to form a polaron near the middle of the polymer chain; (2) at low electric fields, two electrons transfer into the polymer chain to form a bipolaron; (3) at higher electric fields, bipolaron can not be formed in the polymer chain, electrons are transferred from the left electrode to right electrode through the polymer one by one accompanying with

small irregular lattice deformations. This implies that the higher external electric field is disadvantageous for the formation of a bipolaron.

This work was supported by National Natural Science Foundation of China (Nos.90403110, 10374017, 10204005 and 10321003) and the State Ministry of Education of China (No. 20020246006).

References

1. I.H. Campbell, D.L. Smith, Solid State Physics, **55**, 1 (2001) and references therein
2. C.J. Brabec, N.S. Sariciftci, J.C. Hummelen, Adv. Funct. Mater. **11**, 15 (2001)
3. W.P. Su, J.R. Schrieffer, A.J. Heeger, Phys. Rev. Lett. **42**, 1698 (1979)
4. S.A. Brazovskii, N.N. Kirova, Sov. Phys. JETP Lett. **33**, 4 (1981)
5. A.J. Heeger, S. Kivelson, J.R. Schrieffer, W.P. Su, Rev. Mod. Phys. **60**, 781 (1988) and references therein
6. A.R. Brown et al., Chem. Phys. Lett. **210**, 61 (1993)
7. N.C. Greenham et al., Phys. Rev. B **53**, 13528 (1996)
8. S. Brazovskii et al., Optical Materials **9**, 502 (1998)
9. M. Kuwabara, Y. Shimoi, S. Abe, J. Phys. Soc. Jpn. **67**, 1521 (1998)
10. S.J. Xie, J.S. Han, X.D. Ma, Phys. Rev. B **51** 11928 (1995)
11. Z. Xie, Y.M. Kang, Z. An, Y.C. Li, Phys. Rev. B **61**, 1096 (2000)
12. P.S. Davids, A. Saxena, D.L. Smith, Phys. Rev. B **53**, 4823 (1995)
13. Z. An, C.Q. Wu, X. Sun, Phys. Rev. Lett. **93**, 216407 (2004)
14. A.R. Bishop, D.K. Campbell, P.S. Lomdahl, B. Horovitz, S.R. Phillpot, Phys. Rev. Lett. **52**, 671 (1984)
15. Y. Ono, A. Terai, J. Phys. Soc. Jpn. **59**, 2893 (1990)
16. S.V. Rakhmanova, E.M. Conwell, Appl. Phys. Lett. **75**, 1518 (1999)
17. C.Q. Wu, Y. Qiu, Z. An, K. Nasu, Phys. Rev. B **68**, 125416 (2003)
18. J.F. Yu, C.Q. Wu et al., Phys. Rev. B **70**, 064303 (2004)
19. Y.H. Yan, Z. An, C.Q. Wu, Eur. Phys. J. B **42**, 157 (2004)
20. Z. An, C.Q. Wu, Eur. Phys. J. B **42**, 467 (2004)
21. A. Johansson, S. Stafström, Phys. Rev. Lett. **86**, 3602 (2001)
22. A. Johansson, S. Stafström, Phys. Rev. B **69**, 235205 (2004)
23. W.P. Su, J.R. Schrieffer, Proc. Natl. Acad. Sci. U.S.A. **77**, 1839 (1980)
24. M.P. Samanta, W. Tian, S. Datta, J.I. Henderson, C.P. Kubiak, Phys. Rev. B **53**, R7626 (1996)
25. I.H. Campbell, S. Rubin, T.A. Zawodzinski, J.D. Kress, R.L. Martin, D.L. Smith, N.N. Barashkov, J.P. Ferraris, Phys. Rev. B **54**, R14321 (1996)
26. S. Karg, M. Meier, W. Riess, J. Appl. Phys. **82**, 1951 (1997)
27. E.M. Conwell, M.W. Wu, Appl. Phys. Lett. **70**, 1867 (1997)
28. Z.G. Yu, D.L. Smith, A. Saxena, A.R. Bishop, Phys. Rev. B **59**, 16001 (1999)
29. M.-N. Bussac, G. Mamalis, P. Mora, Phys. Rev. Lett. **75**, 292 (1995)